Comparison of Glenohumeral Contact Pressures and Contact Areas After Glenoid Reconstruction With Latarjet or Distal Tibial Osteochondral Allografts

Sanjeev Bhatia,* MD, Geoffrey S. Van Thiel,* MD, MBA, Deepti Gupta,* BS, Neil Ghodadra,* MD, Brian J. Cole,* MD, MBA, Bernard R. Bach Jr,* MD, Elizabeth Shewman,* PhD, Vincent M. Wang,* PhD, Anthony A. Romeo,* MD, Nikhil N. Verma,*† MD, and CDR Matthew T. Provencher,‡ MD, MC, USN
Investigation performed at Rush University Medical Center, Rush Medical College of Rush University, Chicago, Illinois

Background: Glenoid reconstruction with distal tibial allografts offers the theoretical advantage over Latarjet reconstruction of improved joint congruity and a cartilaginous articulation for the humeral head.

Hypothesis/Purpose: To investigate changes in the magnitude and location of glenohumeral contact areas, contact pressures, and peak forces after (1) the creation of a 30% anterior glenoid defect and subsequent glenoid bone augmentation with (2) a flush Latarjet coracoid graft or (3) a distal tibial osteochondral allograft. It was hypothesized that the distal tibial bone graft would best normalize glenohumeral contact areas, contact pressures, and peak forces.

Study Design: Controlled laboratory study.

Methods: Eight cadaveric shoulder specimens were dissected free of all soft tissues and randomly tested in 3 static positions of humeral abduction with a 440-N compressive load: 30°, 60°, and 60° of abduction with 90° of external rotation (ABER). Gleno-humeral contact area, contact pressure, and peak force were determined sequentially using a digital pressure mapping system for (1) the intact glenoid, (2) the glenoid with a 30% anterior bone defect, and (3) the glenoid after reconstruction with a distal tibial allograft or a Latarjet bone block.

Results: Glenoid reconstruction with distal tibial allografts resulted in significantly higher glenohumeral contact areas than reconstruction with Latarjet bone blocks in 60° of abduction (4.87 vs 3.93 cm^2, respectively; $P < .05$) and the ABER position (3.98 vs 2.81 cm^2, respectively; $P < .05$). Distal tibial allograft reconstruction also demonstrated significantly lower peak forces than Latarjet reconstruction in the ABER position (2.39 vs 2.61 N, respectively; $P < .05$). Regarding the bone loss model, distal tibial allograft reconstruction exhibited significantly higher contact areas and significantly lower contact pressures and peak forces than the 30% defect model at all 3 abduction positions. Latarjet reconstruction also followed this same pattern, but differences in contact areas and peak forces between the defect model and Latarjet reconstruction in the ABER position were not statistically significant ($P > .05$).

Conclusion: Reconstruction of anterior glenoid bone defects with a distal tibial allograft may allow for improved joint congruity and lower peak forces within the glenohumeral joint than Latarjet reconstruction at 60° of abduction and the ABER position. Although these mechanical properties may translate into clinical differences, further studies are needed to understand their effects.

Clinical Relevance: Glenoid bone reconstruction with a distal tibial osteochondral allograft may result in significantly improved glenohumeral contact areas and significantly lower glenohumeral peak forces than reconstruction with a Latarjet bone block, which could play a role in improving postoperative outcomes after glenoid reconstruction.

Keywords: glenoid reconstruction; Latarjet; distal tibial allograft

Understanding and properly addressing irregularities in the osseous architecture of the glenohumeral joint are critical to the overall successful treatment of glenohumeral instability.[13,21,22] After a traumatic anterior shoulder dislocation, a concomitant glenoid rim fracture or an attritional bone injury may compromise the static restraints of the glenohumeral joint, further perpetuating shoulder instability. Loss of the glenoid's bony articular conformity significantly inhibits its ability to withstand shear stress.[18]

With recognition of glenoid bone loss as a potential cause for failure in glenohumeral instability, various surgical techniques for glenoid reconstruction have recently been emphasized by many authors, calling attention to this often underappreciated problem.[5,18,19,21,22,29] Principles of surgical management are guided by the extent of osseous injuries to the glenoid, the surgeon's personal experience with specific reconstructive techniques, and patient-specific factors such as work and athletic demands.[22] Both arthroscopic[3,14,15,18,28] and open techniques[2,5,6,24] have been described, and there is a growing body of evidence to suggest that bony reconstruction of the glenoid is recommended if there is significant bone loss (usually >20%-25%).[12,22]

For patients with significant bone defects, several autologous bone grafting procedures, including the Latarjet (and modified Bristow) procedure as well as the use of iliac crest bone grafts, have been described.[11,16,26,29] Although long-term studies have demonstrated that such techniques result in stable and functional shoulders, arthritis continues to be a concern.[8,10,12,20] It is postulated that nonanatomic repair of the glenoid arc, extra-articular nonanatomic repair of capsulolabral tissues, and a lack of chondral surface reconstitution may in part explain the high incidence of degenerative disease after coracoid transfer. In a recent study, Ghodadra et al[8] showed that glenohumeral contact pressures increase by up to 390% in the anteroinferior quadrant of the glenoid when a 30% bone defect is present. The authors then showed that joint contact pressures were optimally restored with flush positioning of an iliac or coracoid bone graft.[8] Coracoid grafts that were placed proud significantly increased peak forces within the joint and altered joint loading patterns, a finding that further supports the rationale for finding anatomic means for reconstruction of a congruous glenohumeral joint.

Reconstruction of glenoid bone defects with distal tibial osteochondral allografts has recently been described as a technique for restoring the articular surface of the glenoid while providing for a customized, anatomic fit of the bone graft and avoiding coracoid morbidity.[24] Although this technique provides the theoretical benefit of improved joint congruity and decreased contact pressures, it is unclear whether the distal tibial graft truly reduces glenohumeral contact pressures and congruity in comparison with coracoid grafts.

The purposes of this study were to determine changes in the magnitude and location of mean contact pressures after (1) the creation of a 30% anterior glenoid defect and subsequent glenoid bone augmentation procedures with flush placement of (2) a Latarjet coracoid graft or (3) a distal tibial
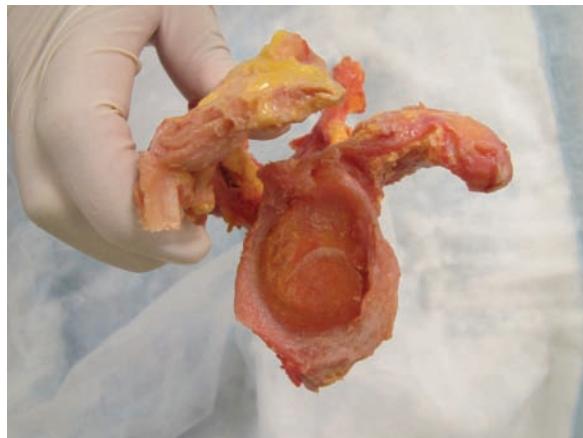
Figure 1. Excluding the labrum, all soft tissues from 8 fresh-frozen human cadaveric shoulders (5 right shoulders and 3 left shoulders from donors with a mean age of 49 years [range, 38-58 years] at the time of death) were dissected, exposing the glenoid.

osteochondral graft. It was hypothesized that bone augmentation with the distal tibial osteochondral graft in a flush position would best normalize articular contact pressures while also providing complete glenoid bone restoration.

MATERIALS AND METHODS

Much of the methodology employed in this study was based on preliminary work by Ghodadra et al.[8] Eight fresh-frozen human cadaveric shoulders (5 right shoulders and 3 left shoulders) from donors with a mean age of 49 years (range, 38-58 years) at the time of death were dissected free of all soft tissues except the labrum (Figure 1). Demographic characteristics of cadaveric shoulder specimens can be found in Table 1. The capsule was sharply excised to expose the humerus and glenoid with the labrum. Before the scapula was potted in a methyl methacrylate block (Isocryl, Lang Dental, Wheeling, Illinois), digital calipers were used to measure the anterior-posterior and superior-inferior diameters of the glenoid with the labrum attached; dimensions were taken based on viewing the glenoid en face as a clock, with the superior portion of the glenoid equivalent to 12 o'clock. Diameters were measured from 12 o'clock to 6 o'clock and from 3 o'clock to 9 o'clock. The height, width (thickness), and length of the corresponding coracoids were also recorded.

†Address correspondence to Nikhil N. Verma, MD, Division of Sports Medicine, Department of Orthopaedic Surgery, Rush University Medical Center, Rush Medical College of Rush University, 1611 West Harrison St, Suite 400, Chicago, IL 60612 (e-mail: nverma@rushortho.com).

*Division of Sports Medicine, Department of Orthopaedic Surgery, Rush University Medical Center, Rush Medical College of Rush University, Chicago, Illinois.

‡Department of Orthopaedic Surgery, Naval Medical Center San Diego, San Diego, California.

TABLE 1
Demographics of Shoulder Specimens (n = 8)

| Demographics	Value
Left shoulder:right shoulder, n	3:5
Age, mean ± SD (range), y	48.6 ± 6.9 (38-58)
Sex, n (%)	
Male	3 (37.5)
Female	5 (62.5)
Cause of death, n (%)	
Myocardial infarction	1 (12.5)
Pneumonia	2 (25)
Hypertensive cardiovascular disease	1 (12.5)
Metastatic skin cancer	1 (12.5)
Melanoma	2 (25)
Lung cancer	1 (12.5)

The scapula was then potted with the glenoid positioned parallel to the floor utilizing a bubble level to ensure that the joint would experience compressive loads rather than shearing forces during testing. Two perpendicular 0.45-inch (11.4-mm) Kirschner wires were inserted through the glenoid neck from the 6-o'clock to the 12-o'clock position and from the 3-o'clock to the 9-o'clock position. These served as reference points to ensure consistent positioning of the pressure sensor pads between trials.

The corresponding humeral shaft was also potted in methyl methacrylate, which was positioned to fit in a custom-designed fixture mounted on a materials testing system (MTS) (Insight 5, MTS Systems, Eden Prairie, Minnesota). Only 2 cm of the proximal part of the humeral shaft was left exposed to minimize diaphyseal bending moments and interference from the testing apparatus during abduction. To define the neutral axis, the bicipital groove was oriented anteriorly, and the humerus was externally rotated 10° (determined with a handheld goniometer), with no applied abduction or flexion.

A 0.1-mm-thick dynamic pressure-sensitive pad (5051 pad, Tekscan, Boston, Massachusetts), with a 56 × 56-mm matrix and a density of 62 sensels/cm^2, was precalibrated with the MTS machine. Calibration was performed per the manufacturer's guidelines, applying loads of 20% and 80% of the maximum test load (440 N) across the glenohumeral joint. For testing, the pressure pad was inserted between the humerus and glenoid, with the 4 quadrants marked on the pad for identical positioning during sequential trials.

Testing Conditions

The MTS machine was used to apply a compressive load of 440 N. A load of 440 N was chosen on the basis of prior work[8] and serves as an approximate maximal load for the simulation of in vivo glenohumeral loading conditions during the range of motion of the shoulder during activities of daily living.[9] Using the Tekscan sensor, the mean glenohumeral contact pressure, contact area, and peak force were determined. The testing sequence included 4 conditions: (1) intact glenoid, (2) glenoid with a 30% anterior bone defect of the glenoid surface area from 2 o'clock to 6 o'clock, (3) a 30% glenoid defect with a Latarjet bone block placed flush with the lateral
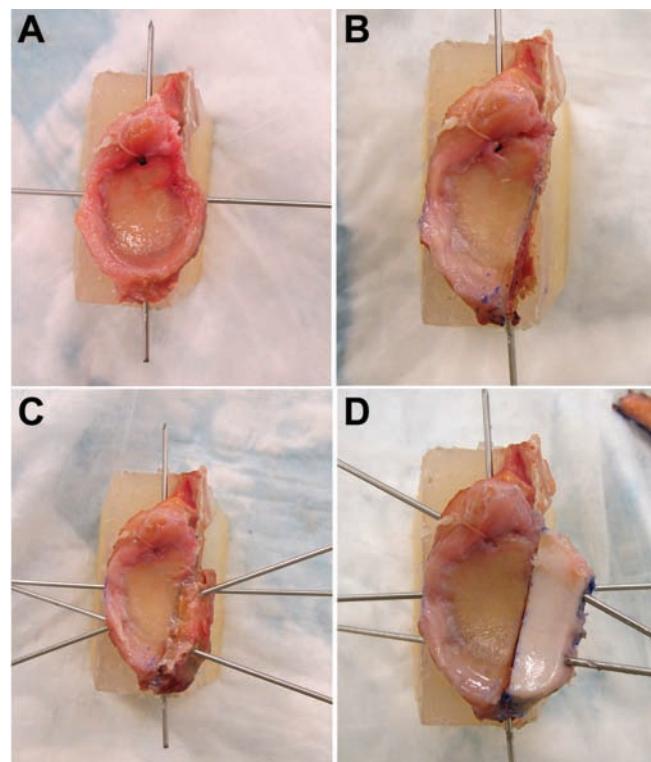

Figure 2. The testing sequence included 4 conditions: (A) an intact glenoid, (B) a glenoid with a 30% anterior bone defect of the glenoid surface area from 2 o'clock to 6 o'clock, (C) a 30% glenoid defect with a Latarjet bone block placed flush with the lateral surface of the coracoid becoming the glenoid face (Latarjet-LAT), and (D) a 30% glenoid defect with a distal tibial bone block placed flush.

surface of the coracoid becoming the glenoid face (Latarjet-LAT), and (4) a 30% glenoid defect with a distal tibial bone block placed flush. An example of a specimen in each of these 4 states is depicted in Figure 2.

The following clinically relevant arm positions were tested for each condition: (1) 30° of humeral abduction with a 440-N load, (2) 60° of humeral abduction with a 440-N load, and (3) 60° of humeral abduction and 90° of humeral external rotation (ABER) with a 440-N load. Such humeral positions of the arm were chosen on the basis of prior work[8] with the hopes of simulating commonly encountered arm positions in a patient with shoulder instability. After each measurement, the pressure sensor was removed and then repositioned according to the previously placed quadrant marks. A new Tekscan sensor was utilized for each specimen.

Bone Defects

An osteotomy simulating 30% bone loss was performed based on a modification of the glenoid bone loss quantification techniques put forth by Sugaya et al[28] and Burkhart et al.[7] As noted in the literature, the amount of glenoid
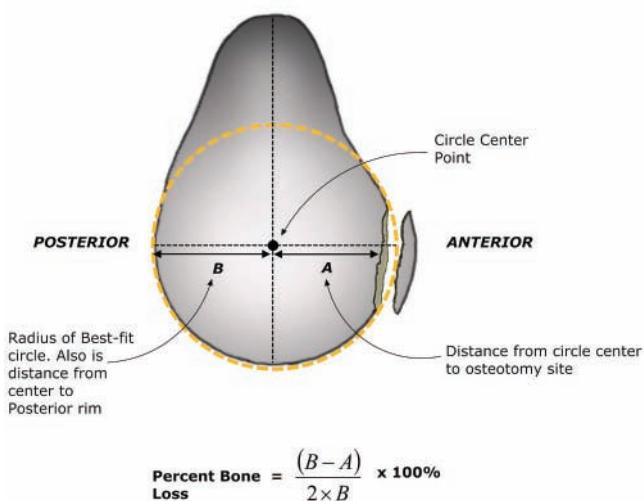
Figure 3. An osteotomy simulating at least 30% bone loss was performed based on a modification of the glenoid bone loss quantification techniques put forth by Sugaya et al[28] and Burkhart et al.[7] As noted in the literature, the amount of glenoid bone loss can be calculated by using the following formula: Defect size = (B − A)/2B × 100%, where "B" is the radius of the glenoid's true-fit circle, and "A" is the distance from the circle center to the edge of the defect. Because defect size was known (in our case, 30%), the formula was rearranged to algebraically solve for "A." For each specimen, the anterior-posterior diameter of the glenoid (2 times the radius, "B") was precisely measured using digital calipers. The distance from the circle center to the osteotomy site ("A") was then solved algebraically. A true-fit circular template was then created with the same diameter as the glenoid specimen and was cut "A" millimeters from the center to replicate the 30% osteotomy site. The template was then applied to the glenoid and oriented such that a clinically relevant osteotomy, one parallel to the long axis of the glenoid, could be created.

bone loss can be calculated by using the following formula: Defect size = (B − A)/2B × 100%, where "B" is the radius of the glenoid's true-fit circle, and "A" is the distance from the circle center to the edge of the defect (Figure 3). Because defect size was known (in our case, 30%), the formula was rearranged to algebraically solve for "A." For each specimen, the anterior-posterior diameter of the glenoid (2 times the radius, "B") was precisely measured using digital calipers. The distance from the circle center to the osteotomy site ("A") was then solved algebraically. A true-fit circular template was then created with the same diameter as the glenoid specimen and was cut "A" millimeters from the center to replicate the 30% osteotomy site. The template was then applied to the glenoid and oriented such that a clinically relevant osteotomy, one parallel to the long axis of the glenoid, could be created. This orientation of the glenoid osteotomy is different from some prior cadaveric studies[9] but is more consistent with clinical bone loss.[23,25,28] Each glenoid osteotomy was
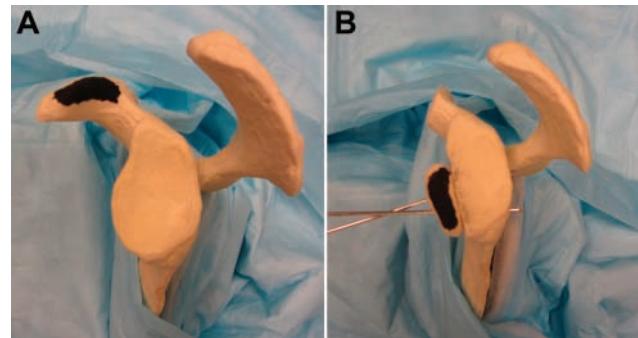

Figure 4. The saw bone model of the glenoid, illustrating how the Latarjet-LAT position was achieved. The coracoid graft was rotated 90° such that the lateral aspect of the coracoid reconstituted the glenoid face and the inferior surface of the coracoid was apposed to the glenoid neck.[26,27] Additionally, the graft was positioned so that the lateral surface was flush with the glenoid face.[8]

made with the use of a 10 × 0.5-mm sagittal saw set to 15,000 revolutions per minute to minimize bone loss. The template remained in place after each osteotomy to ensure that 30% of bone had been removed from the inferior portion of the glenoid. The mean glenoid defect width was 9.2 ± 0.75 mm (standard error of the mean [SEM], 0.26 mm; range, 8-10.5 mm). Before testing, the new anterior-posterior diameter of the glenoid was measured in line with the glenoid bare spot. After each osteotomy, the testing sequence was repeated from neutral to the ABER position, with pressure sensor measurements recorded as described above.

Bone Augmentation Procedures

After the specimen was osteotomized to create a 30% anterior glenoid bone loss model, each of the 8 cadaveric specimens was randomly assigned to first undergo either a Latarjet-LAT autograft procedure or a distal tibial bone graft procedure. For the Latarjet procedure, a mean of 29 mm of the length of the coracoid process was harvested from the cadaveric specimen's coracoid tip to the elbow of the coracoid base. Soft tissue attachments were sharply excised, and the graft's width was recorded. The coracoid graft was rotated 90° such that the lateral aspect of the coracoid reconstituted the glenoid face and the inferior surface of the coracoid was apposed to the glenoid neck (Figure 4).[26,27] Additionally, the graft was positioned so that the lateral surface was flush with the glenoid face.[8] Before fixation, the inferior surface of the coracoid was gently decorticated with the 0.5-mm sagittal saw to replicate the clinical practice of denuding cortical bone on a bone graft for improved healing and incorporation into the glenoid. Two 1.6-mm Kirschner wires, drilled in a nonparallel fashion, were utilized to affix the bone block in place (Figure 4B). A reduction clamp (Synthes, West Chester, Pennsylvania) was used to provide further compression across the construct and prevent subtle changes in position.
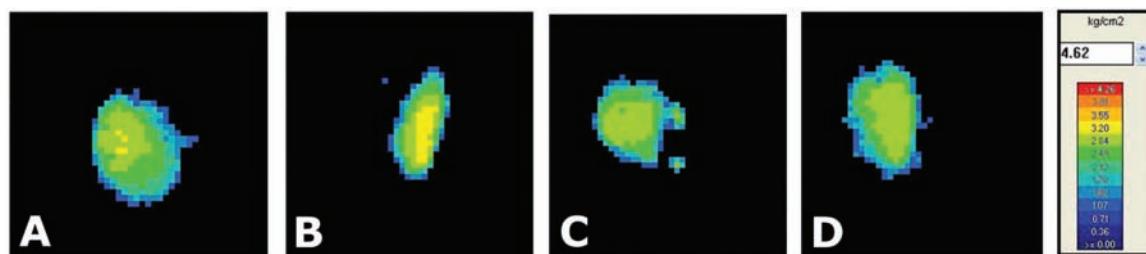
Figure 5. Representative contact pressure map with the arm in 60° of abduction and 90° of external rotation (ABER position). Higher pressures are signified by yellow and orange and lower pressures by blue and green (see scale). (A) Intact glenoid, (B) glenoid with a 30% anterior bone defect (right side), (C) glenoid after Latarjet bone graft procedure, and (D) glenoid after bone reconstruction with a distal tibial allograft.

To perform glenoid augmentation with a distal tibial osteochondral allograft, 8 distal tibial allografts (Allosource, Denver, Colorado) with a mean age of 19.8 ± 3.1 years (range, 16-25 years) were procured. For each glenoid, a distal tibial allograft of the same laterality was utilized for example, right tibias were used for right glenoids and vice versa. As described by Provencher et al,[24] an osteochondral distal tibial graft with the same dimensions as the glenoid defect was carefully cut from the lateral one third of the distal tibia. The graft was appropriately contoured such that it would smoothly align with the natural arc of the glenoid when aligned flush to the articular surface. Like the Latarjet reconstruction, the graft was affixed to the glenoid using two 1.6-mm Kirschner wires, drilled in a nonparallel fashion. A reduction clamp (Synthes) was also used to provide further compression across the construct and prevent subtle changes in position.

Each specimen was tested after both the Latarjet and the distal tibial bone graft procedures in all 3 testing positions. Glenohumeral contact pressure (MPa), contact area (cm^2), and joint peak force (N) were recorded 3 times for each testing condition, with the mean used for data analysis. Contact pressure was defined as the force per unit area of the glenoid. Contact area was defined as the area on which the humerus was able to articulate with the glenoid. Peak force was defined as the highest force recorded within the glenohumeral joint. These data points provided a very revealing snapshot of the physics of glenohumeral articulation.

Statistical Analysis

Data from the pressure and force measurement software, I-scan (Tekscan), were analyzed with descriptive statistics. A repeated 1-way analysis of variance with the Tukey post hoc test was performed using GraphPad Prism 5 software (GraphPad Inc, La Jolla, California) to compare the values between testing conditions. Statistical significance was set to .05.

RESULTS

The mean anterior-posterior diameter of the glenoid specimens was 29.4 ± 3.1 mm (range, 24.5-34 mm). The mean glenoid defect width was 9.2 ± 0.75 mm (SEM, 0.26 mm; range, 8-10.5 mm). The mean width of the tibial grafts was 9.1 ± 0.8 mm (SEM, 0.28 mm; range, 8-10 mm). The mean coracoid thickness (anterior-posterior distance once affixed in the Latarjet-LAT position) before decortication of the inferior surface was 9.5 ± 1.7 mm (SEM, 0.32 mm; range, 7-12.8 mm). In 1 specimen, the coracoid was actually 7 mm thick, much thinner than its corresponding 30% bone defect, which was 9 mm wide. After clinically simulated decortication of this coracoid's inferior surface, this difference was further magnified; the resultant thickness was only 6 mm.

Post hoc power analysis for contact area testing demonstrated that actual power in the 30°, 60°, and ABER groups (effect size of 1.03, 1.25, and 1.36, respectively) was greater than 98% for all. Actual power achieved for the other outcome variable groups was lower; however, confidence can still be expressed in the results because achieving similar power in these testing arms may have been impractical. For instance, to achieve a power of 80% in peak forces for the 30° of abduction group, a sample size of over 662 shoulder specimens would have been required.

Loading of each specimen was successfully performed without any occurrence of fractures, loss of fixation, alterations in abduction position, or equipment failure. Tekscan mapping of glenohumeral contact areas and mean contact pressures demonstrated higher pressures and smaller contact areas in the defect group with subsequent edge loading at the defect site. Overall progression of both contact area and contact pressure from the intact to defect to reconstruction stages with the arm in the ABER position is illustrated in Figure 5.

Contact Area

After the creation of a 30% glenoid defect, measured contact areas for the glenoid face decreased significantly (52%-56%) (Table 2). Glenoid bony reconstruction of the defect with a distal tibial allograft resulted in significantly higher glenohumeral contact areas than reconstruction with Latarjet bone blocks in 60° of abduction (4.87 vs 3.93 cm^2; $P < .05$) and the ABER position (3.98 vs 2.81 cm^2; $P < .05$) (Table 3).

Regarding the bone loss model, distal tibial allograft reconstruction exhibited significantly higher contact areas than the 30% defect model at all abduction positions. Latarjet reconstruction produced significantly higher contact areas

TABLE 2
Normalization (% of Intact State) of Glenohumeral Contact Area, Contact Pressure, and Peak Force[a]

	30° of Abduction			60° of Abduction			ABER		
	Defect	Latarjet	Distal Tibia	Defect	Latarjet	Distal Tibia	Defect	Latarjet	Distal Tibia
Contact area	56.14	74.74	88.04	52.09	73.62	90.4[b]	52.84	71.27[c]	101.4[b]
Contact pressure	115.4	106.97	102.33	116.13	104.61	100.91	115.09	104.48	101.3
Peak force	107.63	101.47	101.28	113.62	108.17	105.28	113.49	109.49[c]	100.4[b]

[a]After creation of a 30% glenoid defect, Latarjet reconstruction, and glenoid reconstruction with a distal tibial osteochondral allograft. ABER, 60° of abduction with 90° of external rotation.
[b]Comparison between distal tibia and Latarjet statistically significant ($P < .05$).
[c]Comparison between defect and Latarjet not statistically significant ($P > .05$).

TABLE 3
Average Values of Glenohumeral Contact Area, Contact Pressure, and Peak Force Obtained
During Tekscan Mapping Trials at Various Humeral Positions

	30° of Abduction			60° of Abduction			ABER		
	Contact Area, cm²	Contact Pressure, kg/cm²	Peak Force, N	Contact Area, cm²	Contact Pressure, kg/cm²	Peak Force, N	Contact Area, cm²	Contact Pressure, kg/cm²	Peak Force, N
Intact glenoid	4.87	2.63	2.36	5.44	2.60	2.23	4.05	2.76	2.35
Defect	2.66	3.05	2.56	2.83	3.04	2.57	2.10	3.19	2.70
Latarjet	3.52	2.83	2.43	3.93	2.73	2.46	2.81[b]	2.90	2.61[b]
Distal tibia	4.20	2.70	2.41	4.87[a]	2.63	2.37	3.98[a]	2.81	2.39[a]

[a]Comparison between distal tibia and Latarjet statistically significant ($P < .05$).
[b]Comparison between defect and Latarjet not statistically significant ($P > .05$).

compared with the bone loss model at only the 30° and 60° of abduction positions (Table 4 and Figure 6A).

Contact Pressure

Regarding measured contact pressures, creation of a 30% bony defect increased mean contact pressures by approximately 15% compared with the intact state in all 3 glenohumeral positions (Tables 2 and 3). Bony reconstruction with both the Latarjet bone blocks and distal tibial allografts significantly lowered mean contact pressures compared with the bone loss model at all abduction positions ($P < .05$) (Table 4). No significant difference in mean contact pressures was found between the Latarjet bone block and distal tibial allograft conditions ($P > .05$) (Figure 6B).

Peak Force

Distal tibial allograft reconstruction demonstrated significantly lower peak forces than Latarjet reconstruction in the ABER position (2.39 vs 2.61 N; $P < .05$) (Table 3). Distal tibial allograft reconstruction produced significantly lower peak forces than the 30% defect model at all abduction positions (Table 4). Latarjet reconstruction also exhibited lower peak forces than the defect model at the 30° and 60° of abduction positions, but differences in peak force between the defect and Latarjet reconstruction in the ABER position were not statistically significant ($P > .05$) (Table 4 and Figure 6C).

DISCUSSION

The principal findings of this study demonstrated that glenoid bone reconstruction with distal tibial allografts resulted in significantly higher glenohumeral contact areas than reconstruction with Latarjet bone blocks at 60° of abduction and at the ABER position. Additionally, distal tibial allograft reconstruction also gave rise to significantly lower glenohumeral peak forces than Latarjet reconstruction in the ABER position. Distal tibial allograft reconstruction exhibited significantly higher contact areas and significantly lower mean contact pressures and peak forces than the 30% defect model at all abduction positions. Latarjet reconstruction also followed this same pattern, but differences in contact areas and peak forces between the defect model and Latarjet reconstruction in the ABER position were not statistically significant ($P > .05$). Thus, even though distal tibial allografts were unable to fully normalize glenohumeral contact areas and contact pressures at all humeral positions, significant differences over Latarjet reconstruction were observed. To our knowledge, this is the first study reported in the literature comparing glenohumeral loading mechanics in a clinically relevant anterior glenoid defect model, a Latarjet reconstruction model, and a distal tibial osteochondral allograft model.

As noted by Greis and colleagues,[9] a 30% glenoid defect increases glenohumeral anteroinferior contact pressures by 300% to 400%, a finding that underscores the need for glenoid reconstruction with adequate bone stock and

TABLE 4
Results of 1-Way ANOVA With Tukey Post Hoc Test[a]

	P Values		
	Defect vs Latarjet	Defect vs Tibia	Tibia vs Latarjet
Contact area			
30°	<.05	<.05	NS
60°	<.05	<.05	<.05
ABER	NS	<.05	<.05
Contact pressure			
30°	<.05	<.05	NS
60°	<.05	<.05	NS
ABER	<.05	<.05	NS
Peak force			
30°	<.05	<.05	NS
60°	<.05	<.05	NS
ABER	NS	<.05	<.05

[a]Note that distal tibial glenoid reconstruction provided significantly increased glenohumeral contact areas as compared with the Latarjet reconstruction at 60° of abduction and at 60° of abduction/90° of external rotation (ABER position). Distal tibial glenoid reconstruction also resulted in significantly less glenohumeral peak forces in the ABER position as compared with the Latarjet model. Distal tibial glenoid reconstruction was significantly superior to the defect model in all testing conditions. The Latarjet reconstruction model was also significantly superior to the defect model in all positions except in ABER. NS, not significant.

appropriate graft choice in patients with such injuries. Open glenoid bone augmentation procedures such as the Latarjet, iliac crest bone grafting, and allograft techniques are currently recommended for any patient with recurrent shoulder instability and greater than 20% to 25% of bone loss. Bone augmentation is necessary in these patients to sufficiently reconstitute the glenoid's osseous arc, one of the key static glenohumeral restraints.[22]

In the Latarjet technique, a locally harvested coracoid autograft is transferred such that it can serve as an extension of the glenoid's articular arc. Although the Latarjet technique was originally described in 1954 and has undergone several variations, little consensus exists on optimal graft orientation.[16,21] In a cadaveric biomechanics study, Ghodadra and colleagues[8] demonstrated that flush positioning of a coracoid graft oriented with its concave undersurface as part of the glenoid arc, the congruent arc modification (Latarjet-INF) as described by Burkhart and De Beer,[5] most optimally restored normal glenohumeral contact pressures and areas. Although such a coracoid orientation has been advocated in the literature, patient-specific and intraoperative factors may sometimes make it difficult to achieve adequate fixation while maintaining the Latarjet-INF orientation. In these instances, the more traditional Latarjet-LAT orientation is frequently substituted.

Despite several decades of evolution in surgical techniques employed during Latarjet glenoid reconstruction, shortcomings in patient outcomes still persist. Currently, concerns regarding coracoid transfer techniques include nonanatomic repair of glenoid defects, poor reconstitution
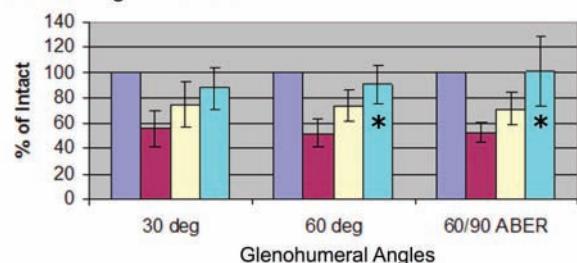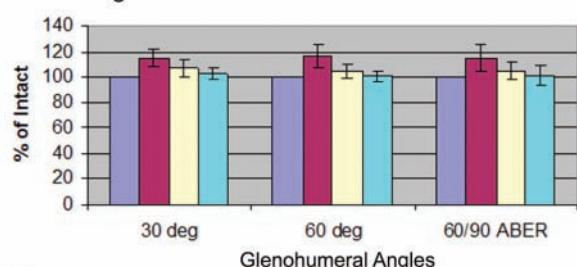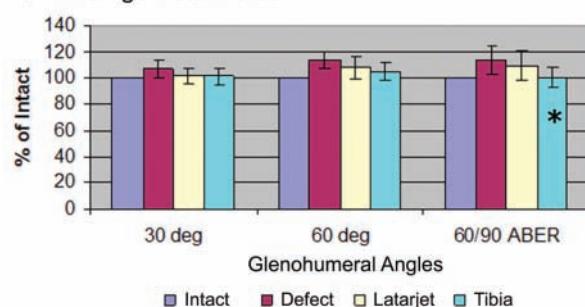
Figure 6. Mean glenohumeral contact area (A), contact pressure (B), and peak force (C) in all 4 states at all 3 positions of the humerus. *Statistically significant difference between the Latarjet reconstruction and the distal tibial allograft reconstruction (P < .05).

of the glenoid arc, extra-articular nonanatomic repair of capsulolabral tissues, and no reconstitution of the chondral surface.[24] Allain and colleagues,[1] in a retrospective review of 58 patients undergoing a Latarjet procedure, found that at a mean follow-up time of 14.3 years, more than half of these shoulders had glenohumeral arthritis, most of which (n = 25) were characterized as grade 1 changes. Other authors investigating outcomes after coracoid transfer procedures have noted comparable findings.[10,12,20] It is hypothesized that the high rate of glenohumeral degenerative changes in this cohort is multifactorial. Certainly, a high degree of chondral injury occurs preoperatively in this group both at the time of initial dislocation but also during subsequent recurrent instability events. However, the results of this study also suggest that intra-articular peak forces may not completely normalize after a coracoid transfer procedure. In fact, in the ABER position, glenohumeral peak forces after Latarjet reconstruction may be more similar to the defect state than an intact glenoid.

Such imperfections in articulation could surely further propagate chondral injuries and elevate joint reactive forces, particularly if joint mechanics are also altered.

Use of distal tibial osteochondral allografts for the reconstitution of glenoid bone defects is a novel technique that capitalizes on the reality that a fresh distal tibial allograft, widely available in tissue banks, contains a robust cartilaginous surface that is highly congruent with the area of glenoid bone loss.[24] Allograft tissue offers all the benefits of avoiding donor-site morbidity that is frequently associated with coracoid transfer or autograft procedures. When comparisons with glenoid allografts are made, a distal tibial allograft is more readily available because the glenoid, a more centrally located structure in the body, is more subject to graft contamination during harvesting. Initial data have shown that the lateral aspect of the distal tibia has a radius of curvature that is quite similar to the glenoid's osseous arc as well as the humeral head.[24] Any subtle differences in curvature can usually be tailored to a precise fit intraoperatively.[24] Moreover, because this tissue source contains dense, weightbearing corticocancellous bone, superb screw fixation can be observed, and the potential for excellent host-graft incorporation exists. Finally, it should be noted that distal tibial allografts allow the reconstitution of actual bone loss as opposed to a limited amount defined by coracoid dimensions. As noted in this study, coracoid thickness was sometimes smaller than the actual amount of bone loss, particularly after clinically simulated decortication of the inferior surface. In these instances, a coracoid graft would not be able to fully restore the glenoid's osseous arc. Bueno and others,[4] in an anatomic study of 31 scapulae, noted that anteroposterior coracoid thickness (thickness of an unaltered coracoid graft in the Latarjet-LAT graft position) was at times only 25% of the corresponding glenoid's width, a finding that complicates glenoid bone restitution in cases with severe defects. Ljungquist and colleagues,[17] in an anatomic study of 100 scapulae, also noted similar findings and concluded that an allograft is generally preferred over a coracoid for larger bone defects, especially when the coracoid graft is proportionately smaller and used in the standard Latarjet-LAT position.

In summary, this is the first biomechanical cadaveric study to compare glenohumeral loading mechanics in a clinically relevant glenoid defect model, a Latarjet reconstruction model, and a distal tibial osteochondral allograft model. In addition to the study design, various strengths of this study include a standardized testing protocol, randomization to different testing arms, and glenoid reconstruction in clinically relevant configurations and patterns.

In spite of identifying important differences between distal tibial and Latarjet glenoid reconstructions, the study is not without some inherent limitations. Perhaps the largest is that a static model of the glenohumeral joint, one devoid of soft tissues, was utilized. Cadaveric tissue does not allow for in vivo evaluation of glenohumeral mechanics, osseous healing, subjective outcomes, or alterations in dynamic constraints in glenohumeral stability after glenoid reconstruction with either the Latarjet technique or distal tibial allografts. Such information would have been

useful particularly because coracoid transfer techniques have the added benefit of creating a sling with the conjoined tendon to oppose anterior humeral translation in the ABER position. A quantitative analysis of the exact location of increased contact pressures was also not performed in part because previously published works using this model demonstrated that contact pressures are primarily increased in the anteroinferior quadrant of the glenoid after the creation of a 30% anterior bone defect.[8] The study's power, although greater than 98% for contact area testing, could also have been improved, particularly for contact pressure and peak force testing. Unfortunately, however, post hoc power analyses demonstrated that achieving similar power in these testing arms would have been impractical given the resources: to achieve a power of 80% in peak forces for the 30° of abduction group, a sample size of over 662 would have been required. The fixation employed for both Latarjet reconstruction and distal tibial allograft reconstruction (multiple, nonparallel Kirschner wires plus a large reduction clamp) was fairly rigid after compression was applied with the clamp; however, it is plausible that a small amount of micromotion may have still been present. Any small degree of micromotion could possibly have affected contact pressure measurements. Cadaveric bone and cartilage are also softer and more predisposed to deformation with excessive load testing. To counteract this limitation, the order in which specimens underwent either a Latarjet or distal tibial glenoid reconstruction (with subsequent testing) was randomized. Tissues were also meticulously kept moist with 0.9% normal saline throughout testing, although the degree of chondrocyte survival in the distal tibial grafts is unknown. Moreover, coracoid grafts, although gently decorticated for improved contouring, were not aggressively reshaped to improve the pressure profile. It is plausible that such a maneuver, although not done clinically, could have altered the observed peak force differences. Finally, it is important to note that our study did not evaluate loading patterns in the congruent arc modification of the Latarjet technique (Latarjet-INF position). Although placing the coracoid in this orientation has been reported to have an improved contact pressure profile than the Latarjet-LAT position, difficulties with fixation have not allowed this technique to be widely utilized in our clinical practice.

CONCLUSION

Principles of surgical management in patients with glenoid bone loss are guided by the extent of the osseous injury, the surgeon's personal experience with specific reconstructive techniques, and patient-specific factors such as work and athletic demands.[22] Open glenoid bone augmentation procedures such as the Latarjet, iliac crest bone grafting, and allograft techniques are currently recommended for any patient with recurrent shoulder instability and greater than 20% to 25% of bone loss. The principal findings of this study indicate that glenoid bone reconstruction with distal tibial osteochondral allografts results in significantly improved glenohumeral contact areas compared with

reconstruction with a Latarjet bone block in 60° of abduction and the ABER position. Additionally, distal tibial allograft reconstruction also results in significantly lower glenohumeral peak forces than Latarjet reconstruction in the ABER position. Further studies are needed to delineate the effects that this improved articulation may have on postoperative outcomes after glenoid reconstruction.

REFERENCES

1. Allain J, Goutallier D, Glorion C. Long-term results of the Latarjet procedure for the treatment of anterior instability of the shoulder. *J Bone Joint Surg Am*. 1998;80(6):841-852.
2. Bigliani LU, Newton PM, Steinmann SP, Connor PM, McIlveen SJ. Glenoid rim lesions associated with recurrent anterior dislocation of the shoulder. *Am J Sports Med*. 1998;26(1):41-45.
3. Boileau P, Bicknell RT, El Fegoun AB, Chuinard C. Arthroscopic Bristow procedure for anterior instability in shoulders with a stretched or deficient capsule: the ''belt-and-suspenders'' operative technique and preliminary results. *Arthroscopy*. 2007;23(6):593-601.
4. Bueno RS, Ikemoto RY, Nascimento LG, Almeida LH, Strose E, Murachovsky J. Correlation of coracoid thickness and glenoid width: an anatomic morphometric analysis. *Am J Sports Med*. 2012; 40(7):1664-1667.
5. Burkhart SS, De Beer JF. Traumatic glenohumeral bone defects and their relationship to failure of arthroscopic Bankart repairs: significance of the inverted-pear glenoid and the humeral engaging Hill-Sachs lesion. *Arthroscopy*. 2000;16(7):677-694.
6. Burkhart SS, De Beer JF, Barth JR, Cresswell T, Roberts C, Richards DP. Results of modified Latarjet reconstruction in patients with anteroinferior instability and significant bone loss. *Arthroscopy*. 2007; 23(10):1033-1041.
7. Burkhart SS, Debeer JF, Tehrany AM, Parten PM. Quantifying glenoid bone loss arthroscopically in shoulder instability. *Arthroscopy*. 2002;18(5):488-491.
8. Ghodadra N, Gupta A, Romeo AA, et al. Normalization of glenohumeral articular contact pressures after Latarjet or iliac crest bone-grafting. *J Bone Joint Surg Am*. 2010;92(6):1478-1489.
9. Greis PE, Scuderi MG, Mohr A, Bachus KN, Burks RT. Glenohumeral articular contact areas and pressures following labral and osseous injury to the anteroinferior quadrant of the glenoid. *J Shoulder Elbow Surg*. 2002;11(5):442-451.
10. Hindmarsh J, Lindberg A. Eden-Hybbinette's operation for recurrent dislocation of the humero-scapular joint. *Acta Orthop Scand*. 1967;38(4):459-478.
11. Hovelius L, Sandstrom B, Sundgren K, Saebo M. One hundred eighteen Bristow-Latarjet repairs for recurrent anterior dislocation of the shoulder prospectively followed for fifteen years, study I: clinical results. *J Shoulder Elbow Surg*. 2004;13(5):509-516.
12. Hovelius LK, Sandstrom BC, Rosmark DL, Saebo M, Sundgren KH, Malmqvist BG. Long-term results with the Bankart and Bristow-Latarjet procedures: recurrent shoulder instability and arthropathy. *J Shoulder Elbow Surg*. 2001;10(5):445-452.
13. Howell SM, Galinat BJ. The glenoid-labral socket: a constrained articular surface. *Clin Orthop Relat Res*. 1989;243:122-125.
14. Kim SH, Ha KI, Kim YM. Arthroscopic revision Bankart repair: a prospective outcome study. *Arthroscopy*. 2002;18(5):469-482.
15. Lafosse L, Lejeune E, Bouchard A, Kakuda C, Gobezie R, Kochhar T. The arthroscopic Latarjet procedure for the treatment of anterior shoulder instability. *Arthroscopy*. 2007;23(11):1242.e1-1242.e5.
16. Latarjet M. [Treatment of recurrent dislocation of the shoulder]. *Lyon Chir*. 1954;49(8):994-997.
17. Ljungquist KL, Butler RB, Griesser MJ, Bishop JY. Prediction of coracoid thickness using a glenoid width-based model: implications for bone reconstruction procedures in chronic anterior shoulder instability. *J Shoulder Elbow Surg*. 2012;21(6):815-821.
18. Mologne TS, Provencher MT, Menzel KA, Vachon TA, Dewing CB. Arthroscopic stabilization in patients with an inverted pear glenoid: results in patients with bone loss of the anterior glenoid. *Am J Sports Med*. 2007;35(8):1276-1283.
19. Montgomery WH Jr, Wahl M, Hettrich C, Itoi E, Lippitt SB, Matsen FA 3rd. Anteroinferior bone-grafting can restore stability in osseous glenoid defects. *J Bone Joint Surg Am*. 2005;87(9):1972-1977.
20. Oster A. Recurrent anterior dislocation of the shoulder treated by the Eden-Hybinette operation: follow-up on 78 cases. *Acta Orthop Scand*. 1969;40(1):43-52.
21. Piasecki DP, Verma NN, Romeo AA, Levine WN, Bach BR Jr, Provencher MT. Glenoid bone deficiency in recurrent anterior shoulder instability: diagnosis and management. *J Am Acad Orthop Surg*. 2009;17(8):482-493.
22. Provencher MT, Bhatia S, Ghodadra NS, et al. Recurrent shoulder instability: current concepts for evaluation and management of glenoid bone loss. *J Bone Joint Surg Am*. 2010;92 Suppl 2:133-151.
23. Provencher MT, Detterline AJ, Ghodadra N, et al. Measurement of glenoid bone loss: a comparison of measurement error between 45 degrees and 0 degrees bone loss models and with different posterior arthroscopy portal locations. *Am J Sports Med*. 2008;36(6):1132-1138.
24. Provencher MT, Ghodadra N, LeClere L, Solomon DJ, Romeo AA. Anatomic osteochondral glenoid reconstruction for recurrent glenohumeral instability with glenoid deficiency using a distal tibia allograft. *Arthroscopy*. 2009;25(4):446-452.
25. Saito H, Itoi E, Sugaya H, Minagawa H, Yamamoto N, Tuoheti Y. Location of the glenoid defect in shoulders with recurrent anterior dislocation. *Am J Sports Med*. 2005;33(6):889-893.
26. Salvi AE, Paladini P, Campi F, Porcellini G. The Bristow-Latarjet method in the treatment of shoulder instability that cannot be resolved by arthroscopy: a review of the literature and technical-surgical aspects. *Chir Organi Mov*. 2005;90(4):353-364.
27. Schroder DT, Provencher MT, Mologne TS, Muldoon MP, Cox JS. The modified Bristow procedure for anterior shoulder instability: 26-year outcomes in Naval Academy midshipmen. *Am J Sports Med*. 2006;34(5):778-786.
28. Sugaya H, Kon Y, Tsuchiya A. Arthroscopic repair of glenoid fractures using suture anchors. *Arthroscopy*. 2005;21(5):635.
29. Warner JJ, Gill TJ, O'Hollerhan JD, Pathare N, Millett PJ. Anatomical glenoid reconstruction for recurrent anterior glenohumeral instability with glenoid deficiency using an autogenous tricortical iliac crest bone graft. *Am J Sports Med*. 2006;34(2):205-212.